IEEE Access
Multidisciplinary : Rapid Review : Open Access Journal

Received December 28, 2019, accepted January 6, 2020, date of publication January 13, 2020, date of current version January 21, 2020.

Digital Object Identifier 10.1109/ACCESS.2020.2966085

A Conditional Symmetric Memristive System With Infinitely Many Chaotic Attractors

JIACHENG GU[1,2], CHUNBIAO LI[1,2,3], YUDI CHEN[1,2], HERBERT H. C. IU[4], (Senior Member, IEEE), AND TENGFEI LEI[3]

[1]Jiangsu Collaborative Innovation Center of Atmospheric Environment and Equipment Technology (CICAEET), Nanjing University of Information Science and Technology, Nanjing 210044, China
[2]Jiangsu Key Laboratory of Meteorological Observation and Information Processing, Nanjing University of Information Science and Technology, Nanjing 210044, China
[3]Collaborative Innovation Center of Memristive Computing Application (CICMCA), Qilu Institute of Technology, Jinan 250200, China
[4]School of Electrical, Electronic, and Computing Engineering, The University of Western Australia, Crawley, WA 6009, Australia

Corresponding author: Chunbiao Li (chunbiaolee@nuist.edu.cn)

This work was supported in part by the National Nature Science Foundation of China under Grant 61871230 and Grant 51974045, in part by the Natural Science Foundation of Jiangsu Province under Grant BK20181410, in part by the Provincial Key Training Programs of Innovation and Entrepreneurship for Undergraduates under Grant 201810300007Z, and in part by the Project Funded by the Priority Academic Program Development of Jiangsu Higher Education Institutions.

ABSTRACT A chaotic system with a hyperbolic function flux-controlled memristor is designed, which exhibits conditional symmetry and attractor growing. The newly introduced cosine function keeps the polarity balance when some of the variables get polarity inversed and correspondingly conditional symmetric coexisting chaotic attractors are coined. Due to the periodicity of the cosine function, the memristive system with infinitely many coexisting attractors shows attractor growing in some special circumstances. Analog circuit experiment proves the theoretical and numerical analysis.

INDEX TERMS Attractor growing, conditional symmetry, hyperbolic function, offset boosting.

I. INTRODUCTION

Memristor as the fourth basic circuit component has raised great interest in nonlinear field. In 1971, Chua predicted the existence of the memristor from the symmetry structure of circuit components. In 2008, HP company developed a solid-state memristor proving the prediction of Chua's. From then on, memristor has been become a research focus in the area of circuit and computer [1]–[4], two main branches of which are physical design and mathematical modeling. Interestingly even hyperbolic sine function [5]–[7], hyperbolic cosine function [8], [9], or even hyperbolic tangent function [10], [11] is used to model memristor for chaos producing.

In addition, multistability of a dynamical system [12], [13] has attracted great interest in nonlinear science and engineering. When the symmetry is broken, symmetric pairs of attractors [6], [14]–[17] are born instead of the symmetric one, even some of which are hidden [18]–[20]. Asymmetric systems give coexisting attractors from different directions. As we know, symmetric attractors can still stay in asymmetric systems when conditional symmetry is obtained [21]. In this case, the polarity balance of conditional symmetry is maintained by the offset boosting. In addition, conditional symmetry provides a new way to organize coexisting attractors [22]–[24], where it is a special bond for attractor growing [25], [26].

In this paper, an offset-boostable chaotic system is selected for hosting memristor and conditional symmetry. By introducing a hyperbolic-tangent-function-based memristor and a cosine function, a new four-dimensional chaotic system was constructed with the following properties: (1) chaos producing; (2) Being of conditional symmetry; (3) Exhibiting infinitely many oscillations; (4) Attractor growing. Therefore, to the best of our knowledge, this class of memristive system has never been reported. In section 2, the newly introduced memristor and the derived chaotic system were given with basic analysis. In section 3, special property of conditional symmetry was analyzed in detail. In section 4, attractor growing was observed. In section 5, circuit experiment proves the theoretical and numerical analysis. Some discussions and conclusions were given in the last section.

The associate editor coordinating the review of this manuscript and approving it for publication was Mohsin Jamil.

II. SYSTEM MODEL

A chaotic system [21] is selected as,

$$\begin{cases} \dot{x} = y^2 - az^2, \\ \dot{y} = -z^2 - by + c, \\ \dot{z} = yz + x. \end{cases} \tag{1}$$

When $a = 0.4$, $b = 1.75$, $c = 3$, system (1) has chaotic solution with Lyapunov exponents (0.1191, 0, −1.2500) and Kaplan-York dimension of $D_{KY} = 2.0953$. A periodic trigonometric function is introduced to coin a self-reproducing system [21],

$$\begin{cases} \dot{x} = y^2 - az^2, \\ \dot{y} = -z^2 - by + c, \\ \dot{z} = yz + d\cos x. \end{cases} \tag{2}$$

When $a = 0.48$, $b = 1.4$, $c = 3$, and $d = 6.2$, system (2) exhibits chaotic oscillation with Lyapunov exponents (0.13966, 0, −1.9466) and Kaplan-York dimension of $D_{KY} = 2.0717$. Since $d\cos(x) = -d\cos(x+(2k+1)\pi)$ ($k \in$ N), when $x \rightarrow x+(2k\pi+1)$ ($k \in$ N), $y \rightarrow y$, $z \rightarrow$ -z, the polarity balance of system (2) is restored, therefore system (2) is of conditional reflection symmetry.

A memristor was selected to maintain the structure of conditional symmetry. The flux-controlled memristor is from a hyperbolic function,

$$\begin{cases} W(w) = \frac{dq(w)}{dw} = \tanh(w), \\ i = W(w)y = \tanh(w)y, \\ \frac{dw}{dt} = y^2 - w. \end{cases} \tag{3}$$

where $W(w)$ represents the voltage and current constraints in the memristor, which is a typical 8-like hysteresis loop. The newly developed memristive system can be rewritten as,

$$\begin{cases} \dot{x} = y^2 - az^2, \\ \dot{y} = -z^2 - by\tanh(w) + c, \\ \dot{z} = yz + d\cos x, \\ \dot{w} = y^2 - w. \end{cases} \tag{4}$$

When $a = 0.5$, $b = 1.4$, $c = 3$, and $d = 6.2$ and the initial conditions are (1, −1, 1, 0) and (1+π, −1, −1, 0), system (4) gives pairs of chaotic oscillations with conditional symmetry with Lyapunov exponents (0.21112, 0, −1.0836, −1.6862), and Kaplan-York dimension$D_{KY} = 2.1948$, as shown in Fig.1. In fact, system (4) exhibits infinitely many chaotic oscillations around those equilibria (0.9788+2$k\pi$, 83.4774, 0.9894, 1.3992) ($k \in$ N) [27]. All those equilibrium points share the same eigenvalues:λ_1 = (−3.4209, 0.86364 ± 2.2862i, −0.30641), showing that they are saddle-foci of index 2.

III. CONDITIONAL SYMMETRY ANALYSIS

Unlike those coexisting symmetric attractors, system (4) also exhibits coexisting attractors of conditional symmetry. The periodic trigonometric cosine function shows the power for generating infinitely many coexisting attractors [28]–[32], as shown in Fig.2.

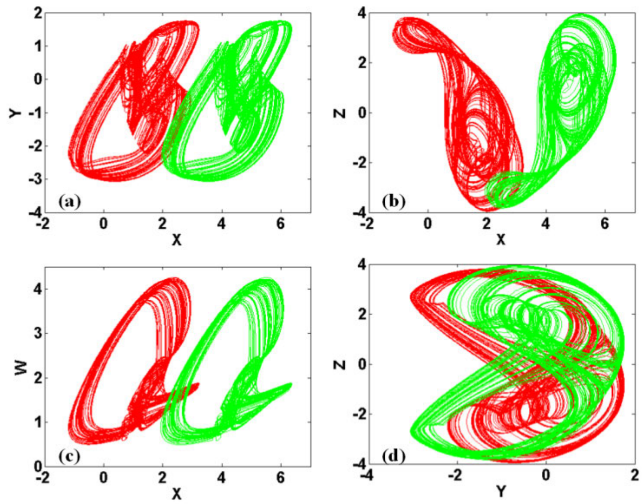

FIGURE 1. Pairs of conditional symmetric chaotic attractors in system (4) with $a = 0.5$,$b = 1.4$, $c = 3$, $d = 6.2$ under initial conditions of [1, −1, 1, 0] and [1+π, −1, −1,0] in red and green respectively: (a) x - y plane, (b) x-z plane, (c) x-w plane, (d) y -z plane.

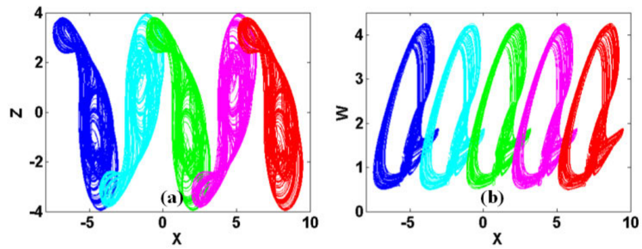

FIGURE 2. Coexisting attractors in system (4) with $a = 0.5$, $b = 1.4$, $c = 3$, $d = 6.2$ under initial conditions [x_0, −1, 1, 0], x_0 = 1, 1+π, 1+2π, 1-π, 1-2π are for green, magenta, red, cyan, blue correspondingly: (a) x-z plane, (b) x - w plane.

By selecting initial conditions, various attractors in their separate basins are extracted. The location of coexisting attractors can be observed from the average value of each variable. As shown in Fig.3(a), when the initial condition of $x \in [-15, 15]$, nine coexisting attractors are captured by the stepwise average value of x. The average value of z sways periodically with the initial value of x proving the conditional reflection symmetric oscillations. Unpredicted jumping of the average value of x indicates the fractal basin boundaries of attraction. Fig.4 shows the unusual "undisciplined jump" when $x_0 = 1.56$, $x_0 = 1.60$ and $x_0 = 1.58$. Different chaotic attractors share the unified Lyapunov exponents, as shown in Fig.3(b). Each coexisting oscillation undergoes its own bifurcation. As shown in Fig.5, when $a = 0.5$, $b = 1.4$, $c = 3$, $d = 6.2$, b varies in [1.35, 1.85], five independent bifurcations coexist safely from different initial conditions of x. All these bifurcations share a unified Lyapunov exponent spectrum approximately.

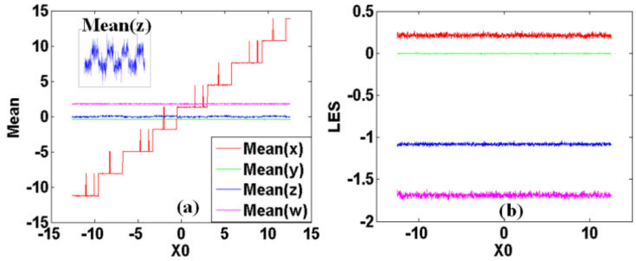

FIGURE 3. Coexisting oscillations in system (4) with $a = 0.5$, $b = 1.4$, $c = 3$, $d = 6.2$ under the initial condition $[x_0, -1, 1, 0]$, $x \in [-4\pi, 4\pi]$: (a) average values of x, y, z, w, (b) Lyapunov exponents.

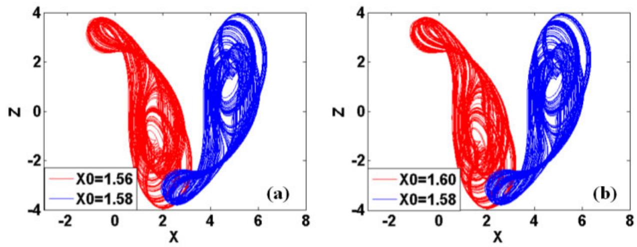

FIGURE 4. Coexisting attractors in system (4) with $a = 0.5$, $b = 1.4$, $c = 3$, $d = 6.2$ under the initial condition $[x_0, -1, 1, 0]$ in the x-z plane.

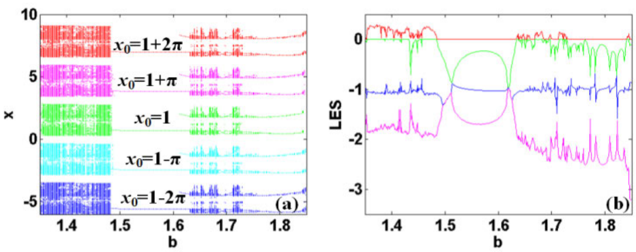

FIGURE 5. Coexisting bifurcations in system (4) with $a = 0.5$, $c = 3$, $d = 6.2$, $b \in [1.35, 1.85]$ under the initial condition $[x_0, -1, 1, 0]$: (a) bifurcation diagram ($y = 0.5$), $x_0 = 1, 1+\pi, 1+2\pi, 1-\pi, 1-2\pi$ are for green, magenta, red, cyan, blue separately, (b) Lyapunov exponent spectra.

When the parameter c varies in [3, 4], system (4) teeters between chaos and periodic oscillation as shown in Fig.6. For the special structure of conditional symmetry, each solution repeats its oscillations in the phase space in pairs. Typical coexisting attractors of conditional symmetry are shown in Fig.7 and Fig.8, the detail information of those solutions are given in Table 1 and Table 2. It is interesting that all these coexisting attractors are arranged in pairs and extend to infinity, but not appear any other kinds of oscillation. And when the parameter c grows bigger, system (4) stays in chaos but without any other style of oscillation. Coexisting pairs of bifurcation of conditional reflection symmetry can be seen in Fig.6 (b).

IV. ATTRACTOR GROWING

Infinitely many attractors may get interlinked when the distance among coexisting attractors get shrined. In this case, computational noise may lead to attractor growing for the

TABLE 1. Coexisting attractors in system (4) with $a = 0.5$, $b = 1.4$, $d = 6.2$.

Cases	parameters	Initial Condition	Lyapunov exponents
Symmetric pair of limit cycles (1-cycle)	$c = 3.24$	0,-1,1,0 π,-1,-1,0	0,-0.55322,-0.92018, -1.3936
Symmetric pair of limit cycles (2-cycle)	$c = 3.655$	0,-1,1,0 π,-1,-1,0	0,-0.11253,-1.0133, -2.1504
Symmetric pair of strange attractors	$c = 3$	0,-1,1,0 π,-1,-1,0	0.20948,0,-1.0833, -1.6842

TABLE 2. Coexisting attractors in system (4) with $a = 0.5$, b f $= 1.4$, $d = 6.2$.

Cases	parameters	Initial Condition	Lyapunov exponents
Symmetric pair of limit cycles (1-cycle)	$c = 3.75$	0,-1,1,0 π,-1,-1,0	0,-0.42605,-1.6061, -1.6061
Symmetric pair of limit cycles (2-cycle)	$c = 3.8$	0,-1,1,0 π,-1,-1,0	0,-0.17931,-0.85772, -2.7138
Symmetric pair of limit cycles (4-cycle)	$c = 3.829$	0,-1,1,0 π,-1,-1,0	0,-0.42531,-0.59724, -2.7274
Symmetric pair of strange attractors	$c = 3.86$	0,-1,1,0 π,-1,-1,0	0.18332,0,-0.96094, -2.9678

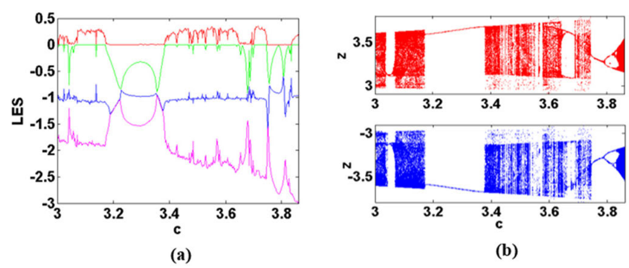

FIGURE 6. Dynamical behavior in system (4) with $a = 0.5$, $b = 1.4$, $d = 6.2$ when $c \in [3, 3.86]$: (a) Lyapunov exponents, (b) bifurcation diagram (cross section: $x = 0$) under the initial condition [0, −1, 1, 0] and [π, −1, −1, 0] are for red and blue.

intertwining of the fractal structure of attraction basin. Otherwise, if the coexisting attractors stand separately with enough

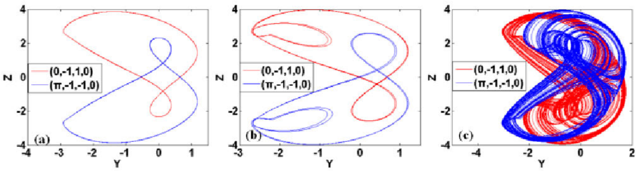

FIGURE 7. Phase portraits of coexisting attractors in system (4) with $a = 0.5$, $b = 1.4$, $d = 6.2$ in the $y-z$ plane: (a) $c = 3.24$, (b) $c = 3.655$, (c) $c = 3$.

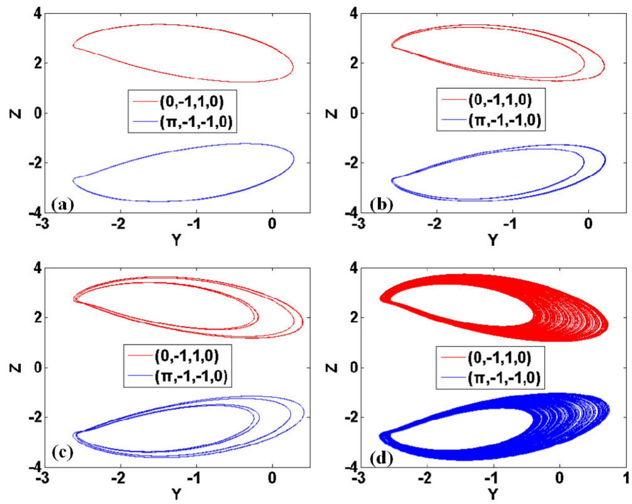

FIGURE 8. Phase portraits of coexisting attractors in system (4) with $a = 0.5$, $b = 1.4$, $d = 6.2$ in the $y-z$ plane: (a) $c = 3.75$, (b) $c = 3.8$, (c) $c = 3.829$, (d) $c = 3.86$.

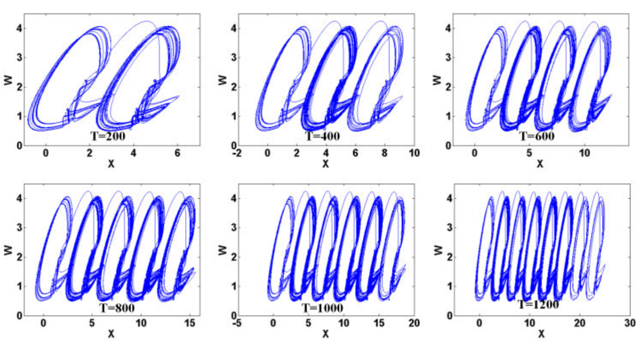

FIGURE 9. Attractor growing of system (4) with $a = 0.45$, $b = 1.54$, $c = 3$, $d = 6.2$ under initial condition $[1, -1, 1, 0]$.

distance, they locate in their basins of attraction safely without any entanglement or interference. In the following, this phenomenon is verified and the corresponding conditions are discussed. As shown in Fig.9, attractor growing was captured in system (4) when $a = 0.45$, $b = 1.54$, $c = 3$, $d = 6.2$ under the initial condition $[1, -1, 1, 0]$. The speed of attractor growing is not even. Two scrolls connect when the time duration T is 200. Another new scroll appears with the time duration of 200 before $T = 1000$. But when T is from 1000 to 1200, two scrolls appear. These linked scrolls have exceeded the definition of a bounded attractor, which can

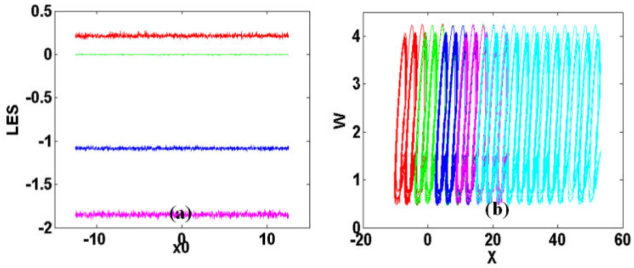

FIGURE 10. Attractor growing under different initial conditions of system (4) with $a = 0.45$, $b = 1.54$, $c = 3$, $d = 6.2$, IC = [f x_0, -1, 1, 0], $x_0 \in [-4\pi, 4\pi]$ under the time duration of $T = 1000$: (a) Lyapunov exponents. (b) Coexisting attractors, and here $x_0 = -4\pi, -2\pi, 0, 2\pi, 4\pi$ are for red, green, blue, magenta, cyan respectively.

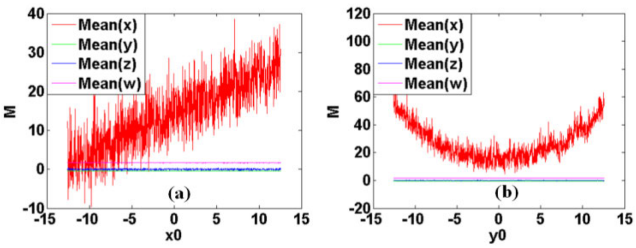

FIGURE 11. Average value evolution of system (4) with $a = 0.45$, $b = 1.54$, $c = 3$, $d = 6.2$ with time duration of $T = 1000$: (a) IC = $[x_0, -1, 1, 0]$, $x_0 \in [-4\pi, 4\pi]$, (b) IC = $[1, y_0, 1, 0]$, $y_0 \in [-4\pi, 4\pi]$.

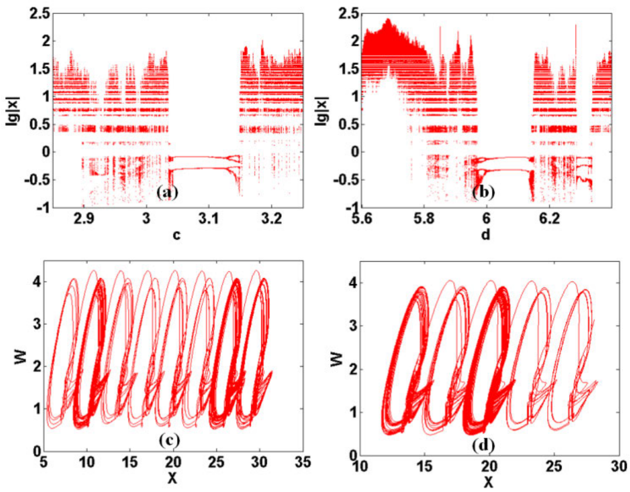

FIGURE 12. Bifurcation diagrams of system (4) with $a = 0.45$, $b = 1.54$, and time duration T f = 1000 under initial condition IC = [1, -1, 1, 0] (cross section of $y = -2$): (a) $d = 6.2$, $c \in [2.85, 3.25]$, (b) $c = 3$, $d \in [5.6, 6.4]$, (c) attractor growing under $c = 3.25$, $d = 6.2$, (d) attractor growing under $c = 3$, $d = 5.85$.

be called as pseudo attractors [25]. Different initial conditions lead to various process of attractor growing reflecting a homogenous multistability. However, all these interlinked attractors share the unified Lyapunov exponents (0.21586, 0, -1.0836, -1.8506) and Kaplan-York dimension of $D_{KY} = 2.1992$, as shown in Fig.10.

Attractor growing in the dimension of x can also be manifested by the evolution of the average value of each

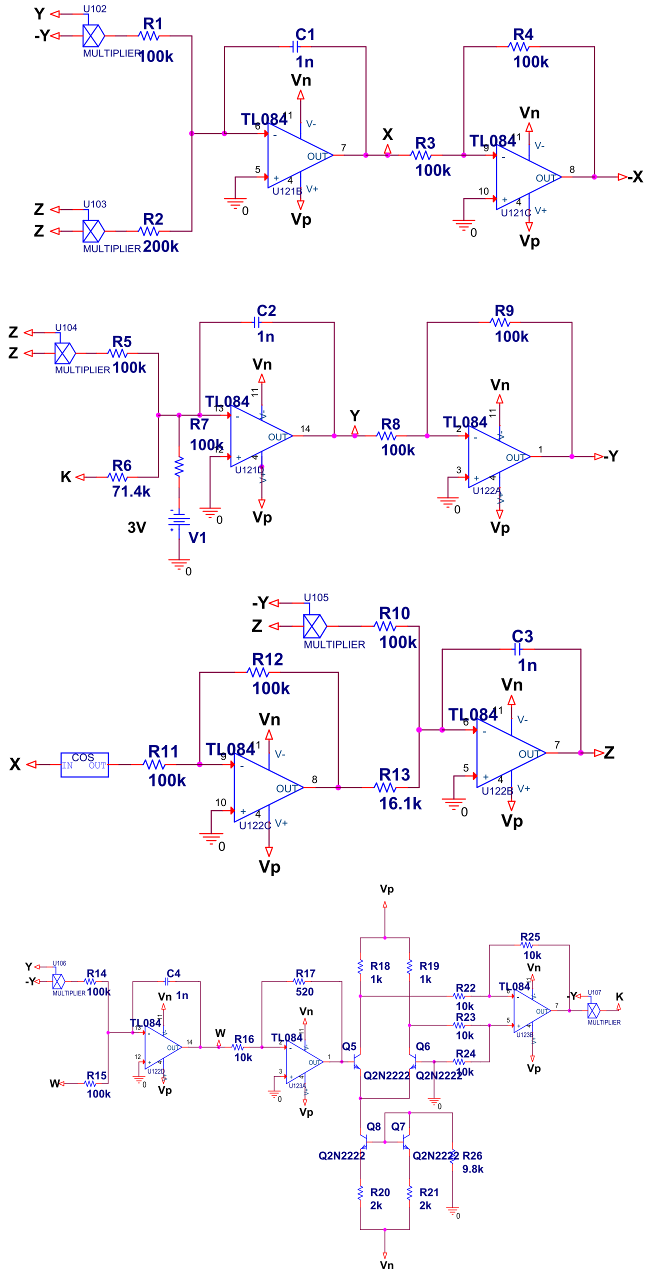

FIGURE 13. Circuit schematic of the memristive system.

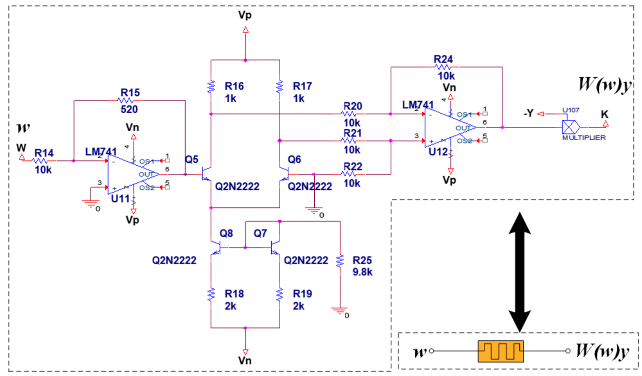

FIGURE 14. Equivalent circuit of the flux-controlled memristor.

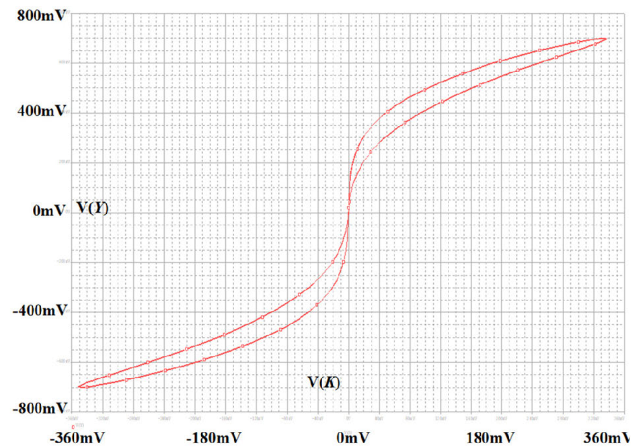

FIGURE 15. Pinched hysteresis loop of memristor *W*(*w*). (f = 200Hz. *x*-axis: 10mv/div, *y*-axis: 50mv/div).

state variable under the continuously revised initial condition. As shown in Fig.11(a), when the initial condition x_0 increases, the average value of x grows almost linearly without considering the influence of computational noise. The average of the other three variables remains almost unchanged. As shown in Fig.11(b), when the initial condition of y_0 continuously grows in $[-4\pi, 4\pi]$, the average value of y, z, and w keeps unchanged, while the average value of x changes in a quadratic way. The reason may be associated with the equation of $\dot{x} = y^2 - az^2$, which implies that the derivative of x is associated with the quadratic function of y and z.

Generally all the bifurcation parameters in the system influence the coexisting bifurcations, and pose a similar effect on attractor growing. As shown in Fig.12(a)(b), when $a = 0.45$, $b = 1.54$, $d = 6.2$, $c \in [2.85, 3.25]$ or $a = 0.45$, $b = 1.54$, $c = 3$, $d \in [5.6, 6.4]$, all the bifurcation diagrams in system (4) show some regions with "zebra-stripe-like bifurcation", where attractor growing can be easily found. The gap of stripes indicates the switches from an attractor to another of conditional symmetry. Since the attractor growing will increase the variable x promptly, here the logarithmic function is applied to low its value so that to scale its growth matching the evolvement of a parameter. The phase trajectories shown in Fig.12(c)(d) proves the attractor growing.

V. CIRCUIT IMPLEMENTATION

Use the PSpice software to simulate the circuit diagram of the system (4). Generally draw a circuit diagram to consider the hardware limitations of the circuit. As is shown in Fig.1, the system variable has a main oscillation in $[-4, 4]$. The analog circuit of system (4) is designed shown

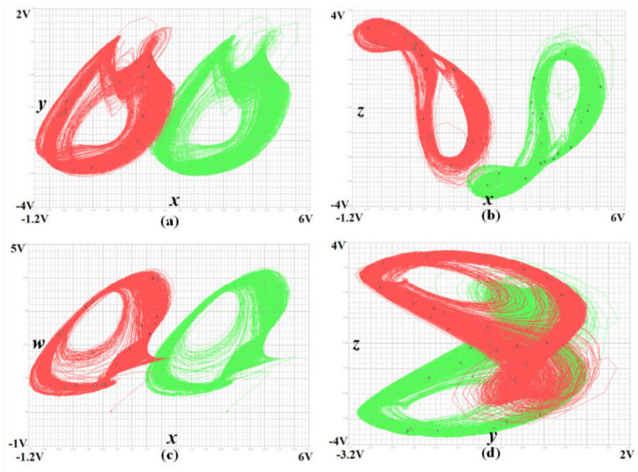

FIGURE 16. **Pairs of conditional symmetric chaotic attractors in system (5) with $a = 0.5$, $b = 1.4$, $c = 3$, $d = 6.2$ under initial condition [1, −1, 1, 0] and [4.14, −1, −1, 0] are for red and green: (a) *x*- *y* (*x*-axis: 0.1v/div, *y*-axis: 0.2v/div), (b) *x*-*z*(*x*-axis: 0.1v/div, *y*-axis: 0.2v/div), (c) *x*-*w*(*x*-axis: 0.1v/div,*y* axis: 0.2v/div), (d) *y*- *z*(*x*-axis: 0.1v/div, *y*-axis: 0.2v/div).**

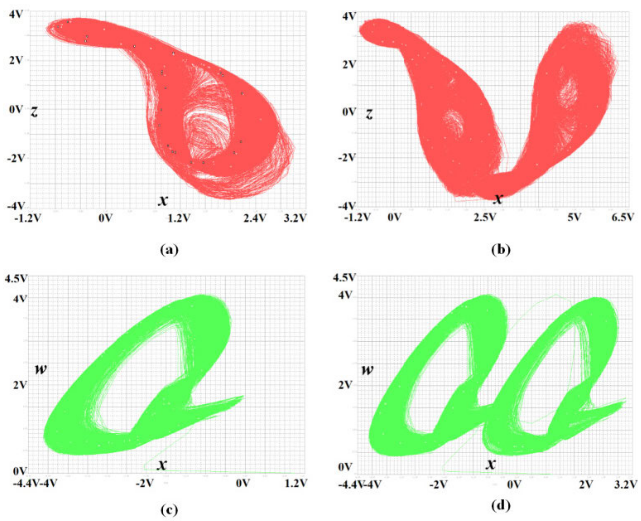

FIGURE 17. **Attractor growing of system (5) with $a = 0.45$, $b = 1.54$, $c = 3$, $d = 6.2$ under the initial condition [1, −1, 1, 0]. (a) *x*-*z* plane with time duration of $T = 5$s (*x*-axis: 0.08v/div, *y*-axis: 0.2v/div), (b) *x*-*z* plane with time duration of $T = 20$s (*x*-axis: 0.1v/div, *y*-axis: 0.2v/div), (c) *x*-*w* plane with time duration of $T = 5$s (*x*-axis: 0.08v/div, *y*-axis: 0.1v/div), (d) *x* -*w* plane with time duration of $T = 20$s (*x*-axis: 0.08v/div, *y*-axis: 0.1v/div).**

in Fig.13 with the circuit equation (5),

$$\begin{cases} \dot{x} = \frac{1}{R_1C_1}y^2 - \frac{1}{R_2C_1}z^2, \\ \dot{y} = -\frac{1}{R_5C_2}z^2 - \frac{1}{R_6C_2}y\tanh(\frac{R_{17}}{2R_{16}V_T}w) + V_1, \\ \dot{z} = \frac{1}{R_{10}C_3}yz + \frac{1}{R_{11}C_3}\cos x, \\ \dot{w} = \frac{1}{R_{14}C_4}y^2 - \frac{1}{R_{15}C_4}w. \end{cases} \quad (5)$$

The circuit consists of four channels that integrate, add, and subtract the state variables x, y, z, and internal variables w, respectively. Addition, subtraction, and integration operations using the operational amplifier TL084 and its peripheral circuits, Ideal multiplier for nonlinear product operations. The variables x, y, z, and w in system (5) correspond to the state voltages of the four channels, respectively. In this circuit, $R_1 = R_3 = R_4 = R_5 = R_7 = R_8 = R_9 = R_{10} = R_{11} = R_{12} = R_{14} = R_{15} = 100\text{k}\Omega$, $R_{16} = R_{22} = R_{23} = R_{24} = R_{25} = 10\text{k}\Omega$, $R_{18} = R_{19} = 1\text{k}\Omega$, $R_{20} = R_{21} = 2\text{k}\Omega$, $R_2 = 200\text{k}\Omega$, $R_6 = 71.4\text{k}\Omega$, $R_{13} = 16.1\text{k}\Omega$, $R_{17} = 520\Omega$, $R_{26} = 9.8\text{k}\Omega$. V_1 is 3V. Select capacitor $C_1 = C_2 = C_3 = C_4 = 1\text{nF}$. Initial voltage of the capacitor $V_{c1} = V_{c3} = 1\text{V}$, $V_{c2} = \text{-}1\text{V}$, $V_{c4} = 0\text{V}$, Stable phase diagram. Derived from [10] in the hyperbolic function $\tanh(\frac{R_{17}}{2R_{16}V_T}w)$, the thermal voltage V_T of the transistor is about 26mV at room temperature. Using a voltage-current exponential characteristic of the collector current of a bipolar NPN transistor to construct a hyperbolic function circuit. The circuit simulation diagram and a plot of pinched hysteresis loop of memristor are shown in Fig.14 and Fig.15. If the voltage across the memristor is v, the current flowing through the memristor is i, a sinusoidal alternating voltage $A\sin(2\pi ft)$ is applied to both ends of the memristor as an excitation signal source with $f = 200$ and amplitude A is 0.7V. When the initial voltage of the capacitor is $V_{c1} = 1\text{V}$, $V_{c2} = -1\text{V}$, $V_{c3} = 1\text{V}$, $V_{c4} = 0\text{V}$ and $V_{c1} = 4.14\text{V}$, $V_{c2} = -1\text{V}$, $V_{c3} = -1\text{V}$, $V_{c4} = 0\text{V}$. The conditional symmetrical chaotic attractors are shown in Fig.16. When the resistance $R_2 = 222.2\text{k}\Omega$ and $R_6 = 64.9\text{k}\Omega$ are changed, attractor growing is shown in Fig.17.

VI. CONCLUSION AND DISCUSSIONS

A hyperbolic-tangent-function-based memristor was introduced in the offset-boostable chaotic system with a cosine function. Infinitely many coexisting attractors of conditional symmetry are produced thereafter. In some circumstances these coexisting attractors link together and finally form attractor growing. Moreover, the initial-condition-induced offset boosting can be produced by other periodic trigonometric functions such as sinusoidal or even tangent function. In this case, the coexisting attractors locate in the basins of attraction with different phases or even periods. Circuit experiment agrees with the numerical simulation proving the unique oscillation in the memristive chaotic system. This unique phenomenon is firstly observed in a memristive system, which deserves further exploration in application engineering.

REFERENCES

[1] C. Li, W. Joo-Chen Thio, H. Ho-Ching Iu, and T. Lu, "A memristive chaotic oscillator with increasing amplitude and frequency," *IEEE Access*, vol. 6, pp. 12945–12950, 2018.

[2] X. Zhong, M. Peng, and M. Shahidehpour, "Creation and circuit implementation of two-to-eight–wing chaotic attractors using a 3D memristor-based system," *Int. J. Circuit Theory Appl.*, vol. 47, no. 5, pp. 686–701, May 2019.

[3] P. Guangya, M. Fuhong, and Y. Biaoming, "Dynamic analysis and circuit implementations of a novel memristive chaotic circuit," in *Proc. 36th Chin. Control Conf. (CCC)*, Nanjing, China, Jul. 2017, pp. 562–567.

[4] B. Muthuswamy and P. Kokate, "Memristor-based chaotic circuits," *IETE Tech. Rev.*, vol. 26, no. 6, pp. 417–432, 2009.

[5] Z. Wang, C. Volos, S. T. Kingni, A. T. Azar, and V.-T. Pham, "Four-wing attractors in a novel chaotic system with hyperbolic sine nonlinearity," *Optik*, vol. 131, pp. 1071–1078, Feb. 2017.
[6] V.-T. Pham, C. Volos, S. T. Kingni, T. Kapitaniak, and S. Jafari, "Bistable hidden attractors in a novel chaotic system with hyperbolic sine equilibrium," *Circuits Syst. Signal Process.*, vol. 37, no. 3, pp. 1028–1043, Mar. 2018.
[7] K. Rajagopal, V.-T. Pham, F. R. Tahir, A. Akgul, H. R. Abdolmohammadi, and S. Jafari, "A chaotic jerk system with non-hyperbolic equilibrium: Dynamics, effect of time delay and circuit realisation," *Pramana*, vol. 90, p. 52, Apr. 2018.
[8] V. F. Signing, J. Kengne, and J. M. Pone, "Antimonotonicity, chaos, quasi-periodicity and coexistence of hidden attractors in a new simple 4-D chaotic system with hyperbolic cosine nonlinearity," *Chaos, Solitons Fractals*, vol. 118, pp. 187–198, Jan. 2019.
[9] K. Rajagopal, S. T. Kingni, G. F. Kuiate, V. K. Tamba, and V.-T. Pham, "Autonomous jerk oscillator with cosine hyperbolic nonlinearity: Analysis, FPGA implementation, and synchronization," *Adv. Math. Phys.*, vol. 2018, pp. 1–12, Sep. 2018.
[10] B. Bao, H. Qian, J. Wang, Q. Xu, M. Chen, H. Wu, and Y. Yu, "Numerical analyses and experimental validations of coexisting multiple attractors in Hopfield neural network," *Nonlinear Dyn.*, vol. 90, no. 4, pp. 2359–2369, Dec. 2017.
[11] X. Hu, C. Liu, L. Liu, J. Ni, and S. Li, "An electronic implementation for Morris-Lecar neuron model," *Nonlinear Dyn.*, vol. 84, no. 4, pp. 2317–2332, 2016.
[12] C. Li and J. C. Sprott, "Multistability in a butterfly flow," *Int. J. Bifurcation Chaos*, vol. 23, no. 12, Dec. 2013, Art. no. 1350199.
[13] C. Li, W. Hu, J. C. Sprott, and X. Wang, "Multistability in symmetric chaotic systems," *Eur. Phys. J. Spec. Top.*, vol. 224, no. 8, pp. 1493–1506, Jul. 2015.
[14] Q. Lai, A. Akgul, C. Li, G. Xu, and Ü. Çavusoglu, "A new chaotic system with multiple attractors: Dynamic analysis, circuit realization and S-box design," *Entropy*, vol. 20, no. 1, p. 12, Dec. 2017.
[15] L. Zhou, C. Wang, and L. Zhou, "A novel no-equilibrium hyperchaotic multi-wing system via introducing memristor," *Int. J. Circ. Theor. Appl.*, vol. 46, no. 1, pp. 84–98, Jan. 2018.
[16] X. Zhang and C. Wang, "A novel multi-attractor period multi-scroll chaotic integrated circuit based on CMOS wide adjustable CCCII," *IEEE Access*, vol. 7, pp. 16336–16350, 2019.
[17] Q. Lai and S. Chen, "Generating multiple chaotic attractors from sprott B system," *Int. J. Bifurcation Chaos*, vol. 26, no. 11, Oct. 2016, Art. no. 1650177.
[18] C. Li and J. C. Sprott, "Coexisting hidden attractors in a 4-D simplified lorenz system," *Int. J. Bifurcation Chaos*, vol. 24, no. 03, Mar. 2014, Art. no. 1450034.
[19] G. A. Leonov, N. V. Kuznetsov, and V. I. Vagaitsev, "Localization of hidden Chua's attractors," *Phys. Lett. A*, vol. 375, no. 23, pp. 2230–2233, 2015.
[20] A. Bayani, K. Rajagopal, A. J. M. Khalaf, S. Jafari, G. Leutcho, and J. Kengne, "Dynamical analysis of a new multistable chaotic system with hidden attractor: Antimonotonicity, coexisting multiple attractors, and offset boosting," *Phys. Lett. A*, vol. 383, no. 13, pp. 1450–1456, Apr. 2019.
[21] C. Li, J. C. Sprott, and H. Xing, "Constructing chaotic systems with conditional symmetry," *Nonlinear Dyn.*, vol. 87, no. 2, pp. 1351–1358, Jan. 2017.
[22] Q. Lai, B. Norouzi, and F. Liu, "Dynamic analysis, circuit realization, control design and image encryption application of an extended Lü system with coexisting attractors," *Chaos, Solitons Fractals*, vol. 114, pp. 230–245, Sep. 2018.
[23] K. Rajagopal, S. Jafari, A. Karthikeyan, A. Srinivasan, and B. Ayele, "Hyperchaotic memcapacitor oscillator with infinite equilibria and coexisting attractors," *Circuits Syst. Signal Process.*, vol. 37, no. 9, pp. 3702–3724, Sep. 2018.
[24] Y.-X. Tang, A. Jalil M Khalaf, K. Rajagopal, V.-T. Pham, S. Jafari, and Y. Tian, "A new nonlinear oscillator with infinite number of coexisting hidden and self-excited attractors," *Chin. Phys. B*, vol. 27, no. 4, Apr. 2018, Art. no. 040502.
[25] C. Li, Y. Xu, G. Chen, Y. Liu, and J. Zheng, "Conditional symmetry: Bond for attractor growing," *Nonlinear Dyn.*, vol. 95, no. 2, pp. 1245–1256, Jan. 2019.
[26] S. He, C. Li, K. Sun, and S. Jafari, "Multivariate multiscale complexity analysis of self-reproducing chaotic systems," *Entropy*, vol. 20, no. 8, p. 556, Jul. 2018.
[27] K. Rajagopal, S. Çiçek , A. J. M. Khalaf, V.-T. Pham, S. Jafari, A. Karthikeyan, and P. Duraisamy, "A novel class of chaotic flows with infinite equilibriums and their application in chaos-based communication design using DCSK," *Zeitschrift Für Naturforschung A*, vol. 73, no. 7, pp. 609–617, Jul. 2018.
[28] C. Li, J. C. Sprott, and Y. Mei, "An infinite 2-D lattice of strange attractors," *Nonlinear Dyn.*, vol. 89, no. 4, pp. 2629–2639, Sep. 2017.
[29] Q. Lai, P. D. K. Kuate, F. Liu, and H. H.-C. Iu, "An extremely simple chaotic system with infinitely many coexisting attractors," *IEEE Trans. Circuits Syst., II, Exp. Briefs*, to be published.
[30] C. Li and J. C. Sprott, "An infinite 3-D quasiperiodic lattice of chaotic attractors," *Phys. Lett. A*, vol. 382, no. 8, pp. 581–587, Feb. 2018.
[31] C. Li, W. Joo-Chen Thio, J. C. Sprott, H. H.-C. Iu, and Y. Xu, "Constructing infinitely many attractors in a programmable chaotic circuit," *IEEE Access*, vol. 6, pp. 29003–29012, 2018.
[32] C. Li, T. Lu, G. Chen, and H. Xing, "Doubling the coexisting attractors," *Chaos*, vol. 29, no. 5, May 2019, Art. no. 051102.

JIACHENG GU is currently pursuing the master's degree in electronics and communication engineering from the Nanjing University of Information Science and Technology, China. His current research interests include memristive systems, and chaotic circuits and their applications.

CHUNBIAO LI received the master's and Ph.D. degrees from the Nanjing University of Science and Technology, in 2004 and 2009, respectively.

From 2010 to 2014, he was a Postdoctoral Fellow of the School of Information Science and Engineering, Southeast University. He was a Visiting Scholar with the Department of Physics, University of Wisconsin–Madison, from 2012 to 2013. He is currently a Professor with the School of Electronic and Information Engineering, Nanjing University of Information Science and Technology. His research interests include the areas of nonlinear dynamics and memristive circuits, including nonlinear circuits, systems, and corresponding applications. He has received several awards for his teaching and research in Jiangsu province.

YUDI CHEN is currently pursuing the bachelor's degree in electronic and information engineering with the Nanjing University of Information Science and Technology, China. His research interests include computer science and circuit design.

HERBERT H. C. IU (Senior Member, IEEE) received the B.Eng. degree (Hons.) in electrical and electronic engineering from The University of Hong Kong, Hong Kong, in 1997, and the Ph.D. degree from The Hong Kong Polytechnic University, Hong Kong, in 2000. In 2002, he joined the School of Electrical, Electronic, and Computer Engineering, The University of Western Australia, as a Lecturer, where he is currently a Professor. He has authored more than 100 articles in his research areas. He has coauthored a book *Development of Memristor Based Circuits* (World Scientific, 2013). His research interests include power electronics, renewable energy, nonlinear dynamics, current sensing techniques, and memristive systems. He has received two IET premium awards, in 2012 and 2014. He has also received the Vice-Chancellor's MidCareer Research Award, in 2014, and the IEEE PES Chapter Outstanding Engineer, in 2015. He currently serves as an Associate Editor for the IEEE Transactions on Circuits and Systems II, the IEEE Transactions on Power Electronics, IEEE Access, the *IEEE Circuits and Systems Magazine*, the *IET Power Electronics*, and the *International Journal of Bifurcation and Chaos*. He serves as an Editorial Board Member of the IEEE Journal of Emerging and Selected Topics in Circuits and Systems and the *International Journal of Circuit Theory and Applications*. He is the Co-Editor of the *Control of Chaos in Nonlinear Circuits and Systems* (Singapore: World Scientific, 2009).

TENGFEI LEI received the M.S. degree in control engineering from Xijing University, Xi'an, China, in 2015. He is currently pursuing the Ph.D. degree in economic chaotic systems with the Rajamangala University of Technology, Rattanakosin, Thailand. He is an Associate Professor with the Qilu Institute of Technology, Jinan, China. His current research interests include fractional order chaotic dynamical systems, chaotic control, and synchronization.